

We are IntechOpen, the world's leading publisher of Open Access books Built by scientists, for scientists

6,900

Open access books available

186,000

International authors and editors

200M

Downloads

Our authors are among the

154

Countries delivered to

TOP 1%

most cited scientists

12.2%

Contributors from top 500 universities



WEB OF SCIENCE™

Selection of our books indexed in the Book Citation Index
in Web of Science™ Core Collection (BKCI)

Interested in publishing with us?
Contact book.department@intechopen.com

Numbers displayed above are based on latest data collected.
For more information visit www.intechopen.com



High Temperature Oxidation Behavior of Thermal Barrier Coatings

Kazuhiro Ogawa

Additional information is available at the end of the chapter

<http://dx.doi.org/10.5772/59794>

1. Introduction

In power generating gas turbine plants, increasing turbine inlet gas temperature (TIT) results in enhancement of turbine efficiency and energy saving. State-of-the-art gas turbine plants aiming at more than 60% turbine efficiency, have to operate at temperature above 1700°C [1, 2]. Therefore, thermal barrier coatings (TBC) have been used in the gas turbine plants for improved durability and performance [3-5]. Typically, the TBC consists of an inner layer of metallic bond coating (MCrAlY, where M indicates Ni, Co, Fe or their combinations) and an outer layer of ceramic top coating (8wt% yttria stabilized zirconia (YSZ)). In the plant, the surface of 1st rotating blades of the gas turbines is exposed to temperature over 900°C. Accordingly, these harsh operational environments may result in degradation such as cracking, delamination, or spalling of the TBC [6]. If the delamination and the spallation occur due to high temperature and long-term operation, serious accidents might break out. Thus, an analysis of the degradation mechanisms of the TBC is important and indispensable in order to prolong service life time. As a result of the delamination or the spallation, Wu et al. [7] suggested that the degradation mechanism is oxidation of the bond coating, coupled with unrelieved coefficient of thermal expansion mismatch stress caused by the pegging effect of protruded bond coating out-grown oxides growing into radial cracks of the top coating. Moreover, Wu et al. [8] described that NiO and Ni(Cr,Al)₂O₄ were observed on both the bottom of the spalled TBC top coating and the outer surface of the MCrAlY bond coating oxide scale after the TBC top coating had spalled on all the test specimens used in their study. This indicates that NiO or Ni(Cr,Al)₂O₄ is the weakest link of the bond coating oxide scale, which might accelerate TBC failure. Bartlett and Maschio [9] expressed that failure of TBC initiated in the thermally grown oxide (TGO) layer is caused by thermal expansion mismatch stresses associated with a nonplanar interface. Furthermore, they reported that crack propagation

occurred in the YSZ top coating in all cases, due to the high fracture energy of the interface. Maier et al. [10] proved that oxidation of the elements of YSZ and MCrAlY reduces the protective capacity of the bond coat during thermal aging. Moreover, both severe degradation of the bond coating and large amounts of nickel oxide have been observed. This nickel oxide was shown to grow outward into the thermal barrier, which appears to result in increase of the stresses in the thermal barrier and contributed to its failure near the interface between YSZ top coat and MCrAlY bond coat. As indicated above, a significant amount of work has been done on the analysis of TBC degradation mechanisms. However, only few attempts have so far been made to investigate TBC degradation associated with TGO growth behavior.

In this chapter, it is described that formation and growth behaviour of the TGO, influence of top coats for formation and growth of the TGO, and improvement of interface strength by controlling TGO morphology.

2. Growth behavior of Thermally Grown Oxide (TGO)

The emphasis has been on failure modes governed by the thermally grown oxide (TGO) [6, 11, 12], predominantly α -Al₂O₃, that forms between the thermal barrier coating (TBC) and the bond coat (see Fig. 1). This thin layer develops large residual compressive stress because of growth and thermal expansion misfit, causing the layer to be unstable against out-of-plane displacements.

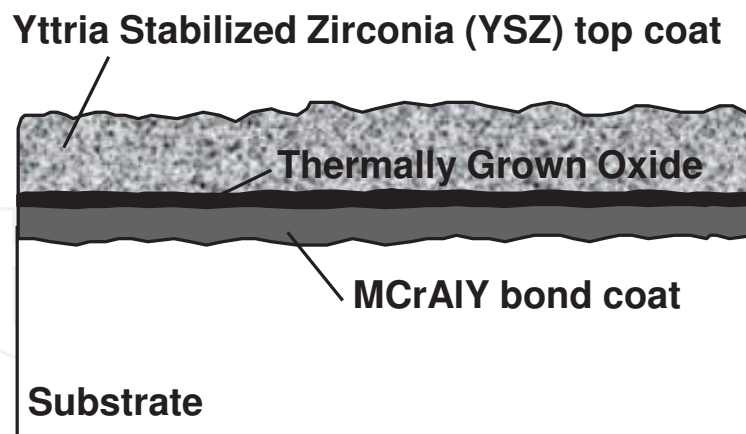


Figure 1. TGO at the interface between top coat and bond coat.

2.1. Experimental procedure

Ni base superalloy was used as a substrate material in this study. The substrate was initially grit blasted, and then positioned into a low-pressure plasma spray (LPPS) coating system for

overlaying of MCrAlY bond coating (approximately 100 μ m thickness). Furthermore, the substrate with MCrAlY bond coating was coated by 8wt% Y₂O₃-ZrO₂ (Yttria Stabilized Zirconia: YSZ) TBC top coating (approximately 300 μ m thickness) by an air plasma spraying (APS) coating system.

The specimens were uniformly aged at 1000°C by using high temperature furnace in the ambient air. The reason for the choice of 1000°C was to simulate the surface temperature of the first rotating blades of 1500°C class gas turbine plants. The coated specimens were aged at 1000°C for various lengths of time viz, 10, 50, 100, 500, 1000 and 3000 hours. The aged specimens were compared with as-received specimen due to investigation of an extent of degradation. Before aging, the TGO was identified at the TBC/MCrAlY interface. On the other hand, in the case of the aged specimens, TGO formation was confirmed.

In order to understand the relationship between the aging time and the growth of TGO layer, cross-section of thermally aged specimens was characterized with use of scanning electron microscope (SEM). The thickness, porosity, and microcracks of TGO layer for the specimens were measured at over 50 points by using SEM. Furthermore, due to identification of chemical composition of the TGO, analyses were using energy dispersive X-ray spectroscopy (EDX) and electron probe micro analyzer (EPMA) performed.

2.2. Results and discussion

2.2.1. Observations and identifications of thermally grown oxide

SEM observation gave information on the initial degradation such as microcracks, pores, and TGO as well as microstructure. Typical SEM images of TBC of as-received and 3000hours thermally aged specimen are shown in Fig.2. Moreover, typical SEM images of the cross-section in the vicinity of the TBC/MCrAlY interface are displayed in Fig.3. It is confirm that the TGO is formed at TBC/MCrAlY interface. Furthermore, the TGO layer has irregular shape and its thickness varies at the TBC/MCrAlY interface. This TGO layer contains at least two layers with different color contrasts on SEM images. There is black layer closer to the bond coating, and gray layer near the YSZ. Observation of the TGO layer at higher magnification, Fig.3, reveals that there are many pores, especially in the gray layer.

Energy dispersive X-ray spectroscopy (EDX) analysis was performed in order to investigate the chemical composition of the black and the gray layers. The results of the EDX analysis are presented in Fig. 4. It turns out that the black layer in Fig.4 contains only Al and O.

Consequently, the black layer is identified as Al₂O₃ (Alumina). The EDX spectrum of the gray layer contains various peaks of Al, O, Co, Cr and Ni, suggesting that the layer can be a mixed oxide consisting of a combination of NiO, CoO, Cr₂O₃, Ni(Cr, Al)₂O₄ spinels. Since the composition of the gray layer is not well defined, it will be referred to as mixed oxide layer in this work.

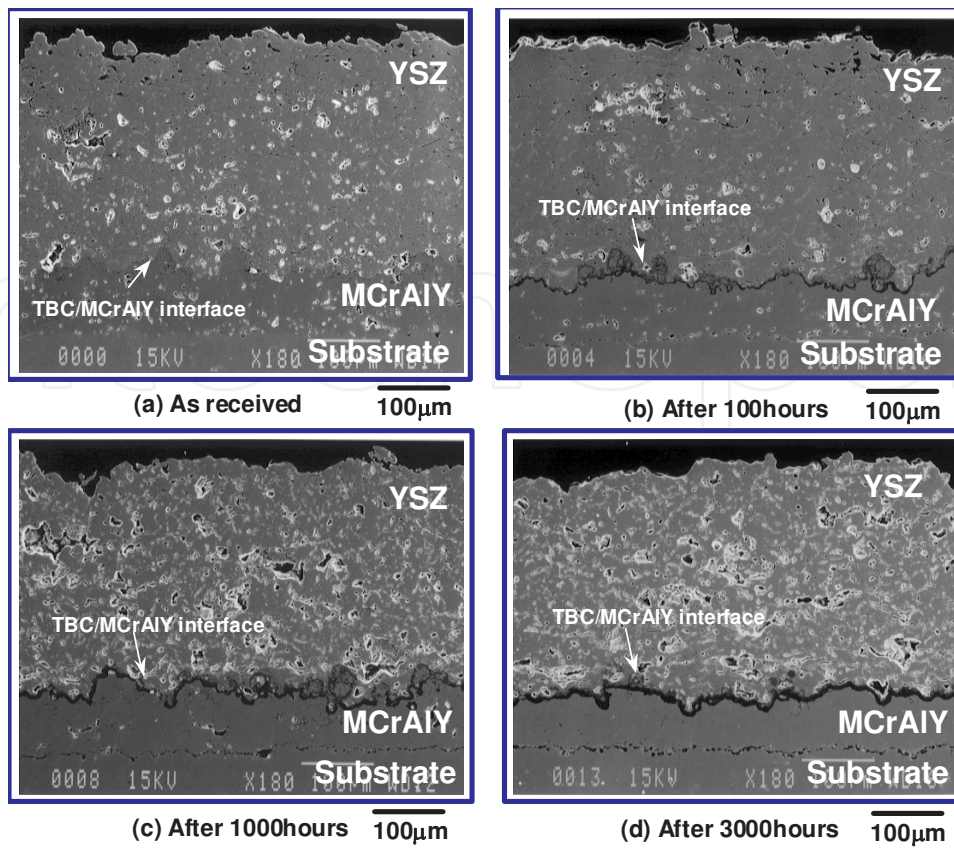


Figure 2. Typical SEM images of the cross-sections of TBC.

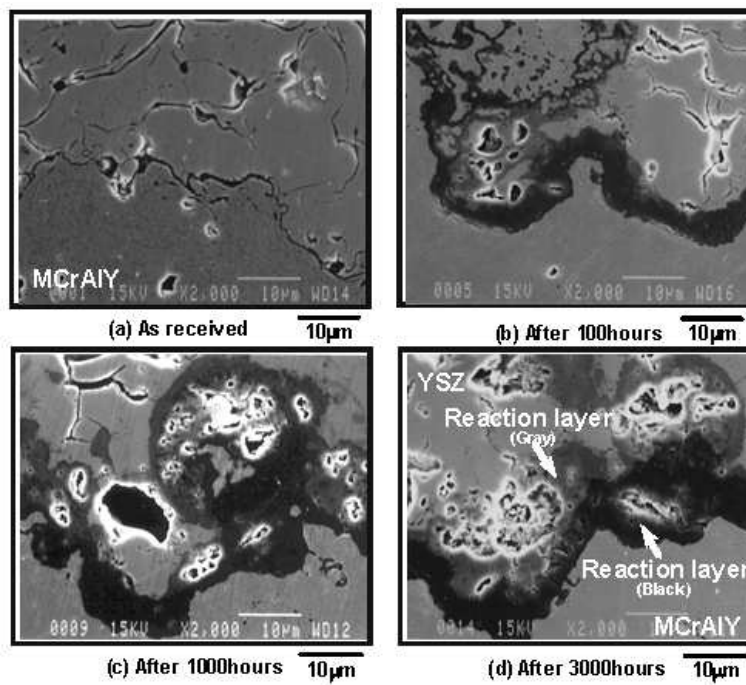


Figure 3. Typical SEM images of the cross-sections in the vicinity of the TBC/MCrAlY interface.

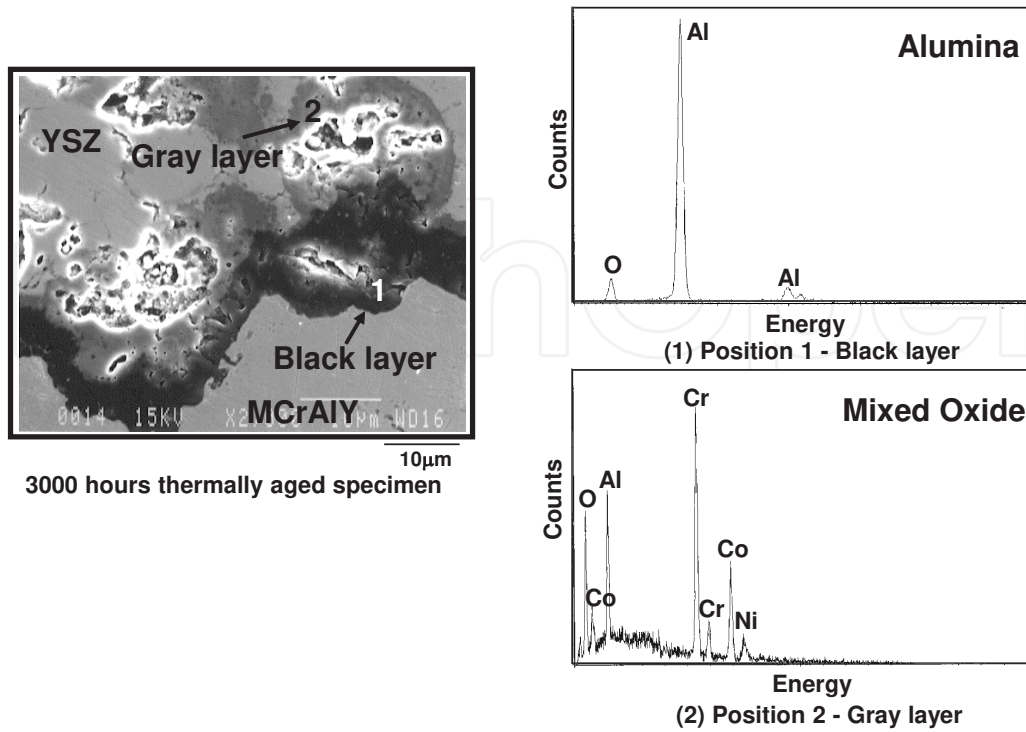


Figure 4. Results of EDX analysis.

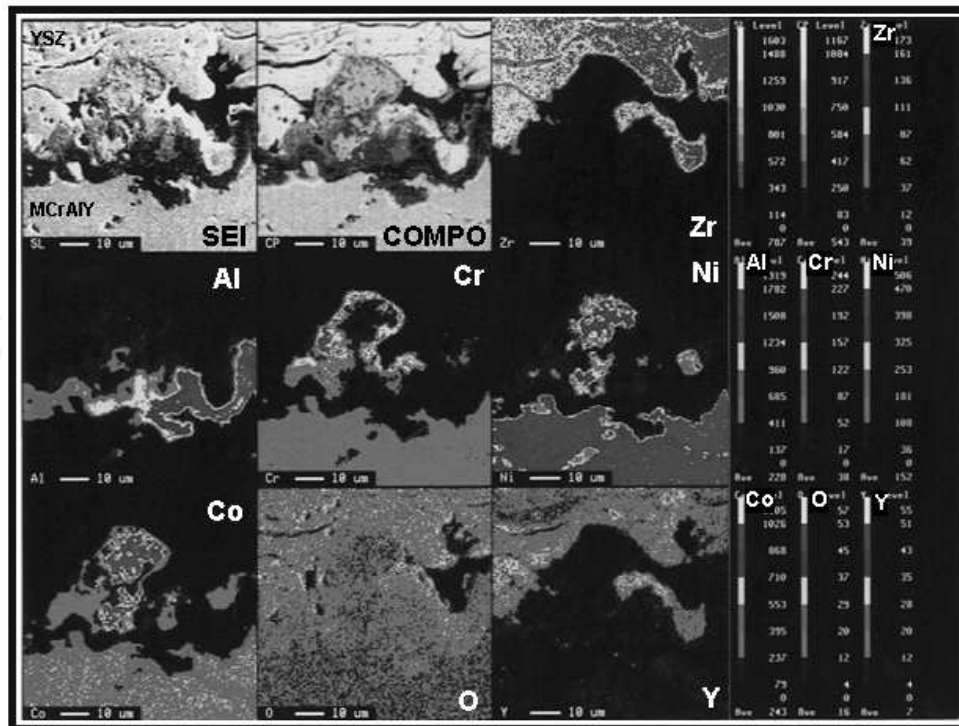


Figure 5. EPMA analysis of the cross-section of TBC/MCrAlY interface.

In addition, EPMA elemental mapping was carried out due to identify the alumina and mixed oxide in detail. The result of EPMA analysis is shown in Fig.5. In black layer, only O and Al are present as it was displayed in Figs.2 and 3. Namely, the black layer was identified as Alumina. However, there is hardly any Al in MCrAlY bond coating. It is supposed that almost all Al in the MCrAlY is combined with oxygen forming alumina at the interface. In case of mixed oxide, Cr-rich layer was identified at outer of the oxide. On the other hand, Co and Ni-rich phase were found in inside of mixed oxide. As a result, it is thought that the outer of the mixed oxide is chromium oxide (Cr_2O_3), and the inner of the mixed oxide is CoO, NiO, or spinels.

2.2.2. Oxidation process of TGO

It is important to evaluate the oxidation behavior of TGO (alumina layer and mixed oxide layer) for prediction of remaining life time of TBC. Accordingly, we investigated thickness growth of alumina and mixed oxide layer in dependence on aging time. The relationship between average thickness of each layer and aging time is shown in Fig.6.

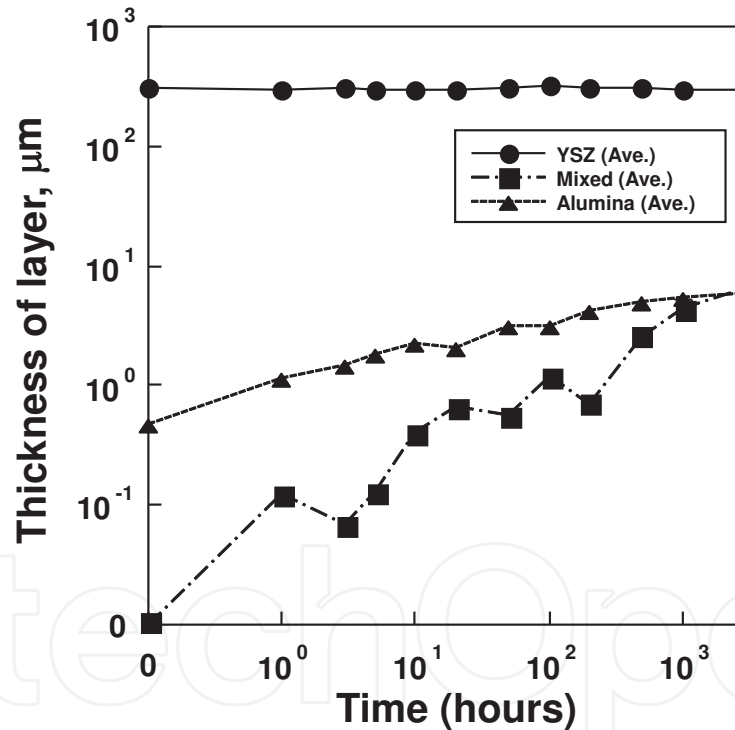


Figure 6. Variation of thickness of each layer with aging time.

The YSZ layer as top coating has scarcely thickness variation in spite of increasing aging time. On the other hand, it is clearly visible that longer aged specimens contain thicker TGO layer, and the TGO layer gradually increases with aging time. For short aging time, the TGO is predominantly alumina rather than mixed oxide. However, when the thermal aging exceeds 1000 hours, the thickness of the mixed oxide layer becomes similar to that of the alumina layer due to significant increase of the thickness of the mixed oxide layer.

Relationship between TGO thickness and square root of time is depicted in Fig.7. From this figure, it is determined that the growth of mixed oxide obeys parabolic law. Therefore, the mixed oxide is protective film in spite of having many pores. On the other hand, the alumina thickness cannot be expressed in terms of a parabolic law in this study. Generally, it is known that alumina monolayer obeys parabolic law [13], however, the oxidation rate of alumina decreases as the thickness of mixed oxide increases due to the formation of protective mixed oxide over the alumina layer. It is thought that protective mixed oxide has an effect on penetration of oxygen or on reduction of oxygen potential. The oxidation rate constant k_A of alumina can be expressed as a function of the thickness of mixed oxide.

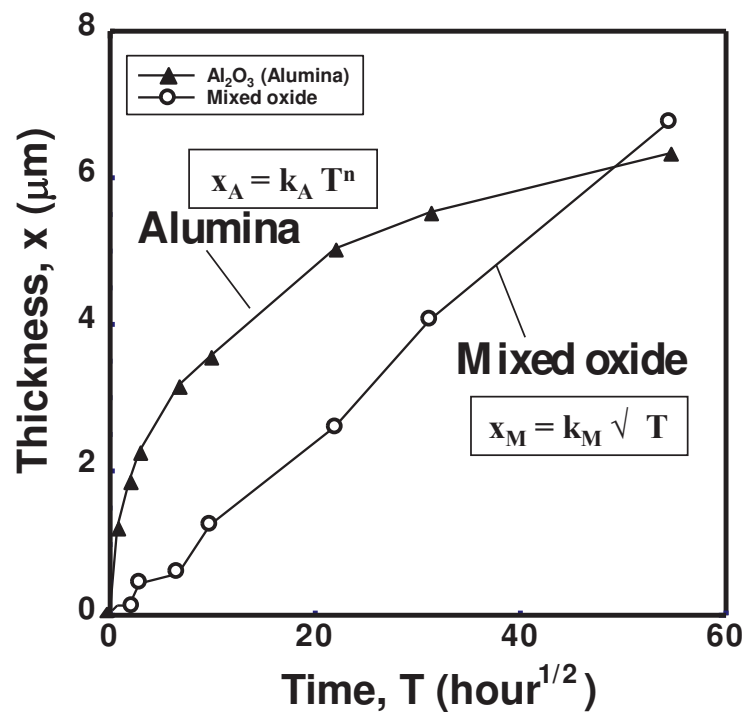


Figure 7. Relationship between TGO thickness and square root of time.

The thickness of the mixed oxide, x_M , and the alumina, x_A , can be expressed as follows:

Mixed oxide layer:

$$x_M = k_M \sqrt{T} = 0.125 \sqrt{T} \quad (1)$$

Alumina layer:

$$x_A = 1.29 T^{0.21} = k_A (x_M) \sqrt{T} = 0.388 x_M^{-0.580} \times \sqrt{T} \quad (2)$$

where T is aging time, k_M and k_A are oxidation rate constant of mixed oxide and alumina, respectively.

It is assumed in Eq. (2) that the alumina thickness obeys anomalous parabolic law. As a result, the calculated value corresponded to the experimental value very well. Furthermore, it has been made clear that oxidation behavior of the mixed oxide layer obeys parabolic law. On the other hand, it is thought that the oxidation rate constant of the alumina is a function of thickness of mixed oxide.

2.2.3. Variation of microcracks and porosities for each layer

In case of formation of defects such as microcrack or porosity in the aged TBC specimen, these defects increase with stress in the vicinity of the tip. Accordingly, it is thought that macrocrack or delamination initiate from tip of these defects. There are some microcracks and porosities in the YSZ and TGO layer of aged specimens in this study. Consequently, the influence of increase in porosity and microcrack was investigated. The relationship between ratio of porosity and microcrack is displayed in Fig.8. The porosities and the microcracks ratio are drastically increasing after more than 500 hours aging. The amount of the porosities and the microcracks in the each layer increased with aging time. Especially, the microcrack in the YSZ top layer is notably increased. Moreover, the porosities in the mixed oxide are remarkably formed. On the other hand, there is no remarkable increase in the porosities and the microcracks of the alumina layer. Normally, it is thought that YSZ layer decreases the porosity and the microcrack in inner of this layer due to sintering. However, countless porosity and microcrack in the YSZ layer are formed due to thermal expansion mismatch accompanied with formation and growth of TGO. Moreover, it is thought that formation of numerous porosities in the mixed oxide is caused by Kirkendall porosity [14] due to difference in diffusion rates. The increasing porosities ratio is result of condensation of the porosities during thermal exposition.

2.2.4. Formation of the macrocracks

It is thought that the macrocracks and delamination in the YSZ were caused by the increasing amount of the porosity and microcrack. Correspondingly, the interface between TBC and MCrAlY was observed for the long-term aged specimen. The example of observation in the vicinity of the interface is shown in Fig.9. In case of 500 and 1000 hours aged specimens, there is almost no macrocrack in the vicinity of the interface. However, in case of 3000 hours aged specimen, the macrocrack was detected at everywhere in the TGO. The macrocrack passed through the porosity of the mixed oxide or the microcrack of the YSZ. Furthermore, the macrocrack grew to vertical direction of the thickness. It is supposed that a reason for the formation of the macrocrack only in case of the long-term aged specimen is increase in thermal stress accompanied by thermal expansion mismatch due to increasing thickness of the alumina. This effect can be one of driving forces of delamination and macrocrack formations. However, the driving force is not only thermal stress but also decreasing bonding force or formation of stress concentration site caused by formation of porosity or microcrack. Almost all macrocracks passed through the porosity in mixed oxide or microcrack in YSZ layer.

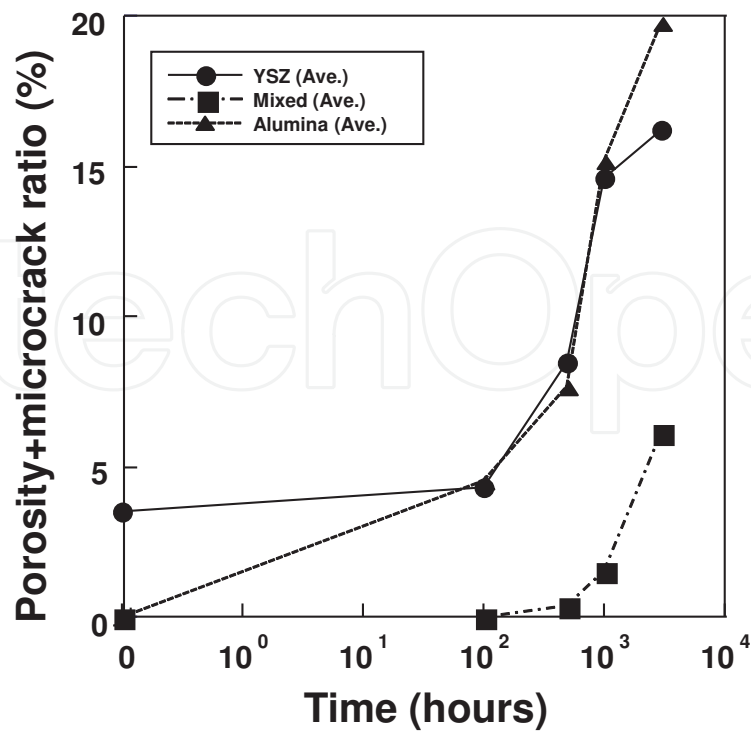


Figure 8. Time dependence of porosity and microcrack ratio.

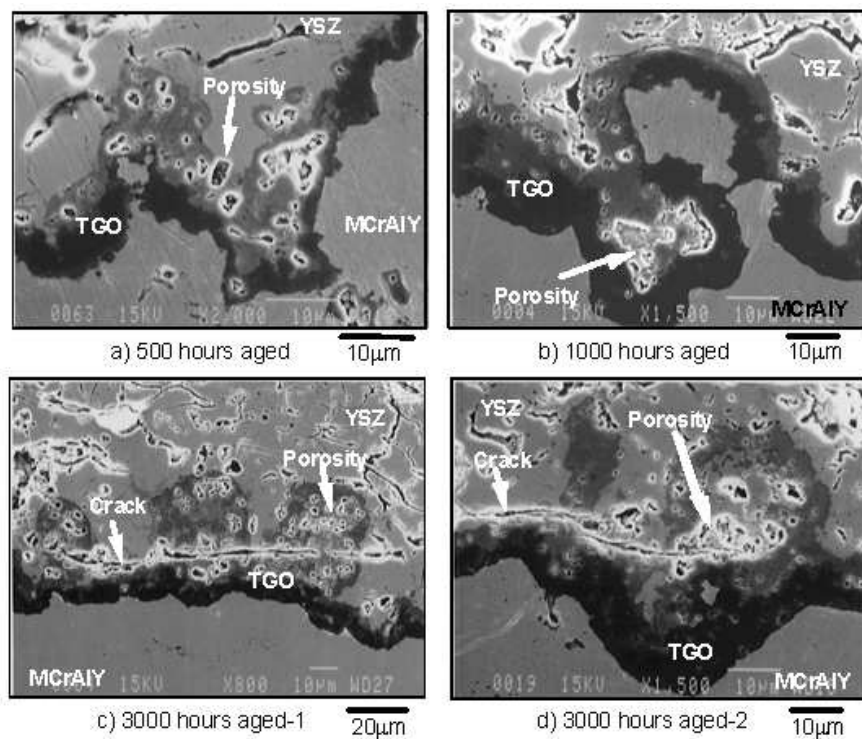


Figure 9. Macrocracks in the vicinity of TBC/MCrAlY interface.

The microcracks were formed everywhere inside of YSZ. This means that there is some possibility of initiating macrocrack from the all of microcracks. However, almost all macrocracks were formed in the vicinity of the YSZ/MCrAlY interface, which is supposed to be caused by thermal expansion mismatch in the part close to interface.

2.3. Summary

The kinetics of thermally grown oxide at interface between TBC and MCrAlY was investigated. Moreover, the driving force of macrocracks formation was suggested. The following conclusions are drawn:

During thermal aging, a TGO is formed at the TBC/MCrAlY interface. SEM and EDX analysis show that the TGO contains two different oxide films. One is alumina closer to the MCrAlY, and the other one is mixed oxide closer to the TBC.

Thickness of both alumina and mixed oxide increased with aging time. On the other hand, the YSZ layer as top coating has scarcely thickness variation in spite of increasing aging time.

The thickness of mixed oxide film obeys parabolic law, and the mixed oxide is protective film in spite of having many porosities. On the other hand, the alumina thickness cannot be expressed by parabolic law. The oxidation rate of alumina decreases, which is accompanied by increasing thickness of mixed oxide increases, due to the formation of protective mixed oxide over the alumina layer. Correspondingly, it is assumed that the alumina thickness obeys anomalous parabolic law.

In the case of 500 and 1000 hours aged specimens, there is no macrocrack in the vicinity of the interface. However, in case of 3000 hours aged specimen, the macrocrack was identified everywhere in the TGO. This reason indicates that thermal expansion mismatch accompanied by formation and growth of alumina is one of the driving forces of macrocracks formation. However, the driving force is not only thermal stress but also decrease in adhesive force or formation of stress concentration site caused by formation of porosity or microcrack. Almost all macrocracks passed through the porosity in mixed oxide or microcrack in YSZ layer.

It is thought that the delamination or the spalling is initiated and propagated due to an interaction of these degradation factors such as thermal stress, initiation of stress concentration sites, and decreasing adhesive force due to formation and growth of alumina, porosities and microcracks.

3. Influence of top coats for formation and growth of the TGO

During exposure to high temperatures, thermally grown oxide (TGO) forms at the interface between the top-coat and bond-coat as has mentioned in previous section. However, there is almost no investigation on the influence of YSZ top coat for formation and growth of the TGO. Therefore, in order to understanding existence of the YSZ top coat on TGO growth, specimens with and without YSZ top coat are compared.

3.1. Experimental

3.1.1. Specimens

Two kinds of specimens are prepared. One is a specimen with TBC; the other is a specimen without TBC. Regarding other factor such as thermal spraying condition, used powders for spraying, used material, environment, both specimens are indiscernible. In both specimens, Tomilloy, Ni base superalloy, is used as a substrate material. These two kinds of specimens are used for examining the microstructural and compositional changes and microcracks formation in the oxides at TBC/MCrAlY interface region for the specimen with TBC, and MCrAlY surface for the specimen without TBC. Analysis was performed using scanning electron microscope (SEM), energy dispersive X-ray spectroscopy (EDX), and electron probe micro analyzer (EPMA).

The substrate is grit blasted initially, and then positioned into a LPPS system for overlaying of CoNiCrAlY bond coating (approximately 100 μ m thickness). In case of the specimen with TBC, the YSZ-TBC top coating (approximately 300 μ m thickness) is further coated using an APS system. The geometry of the tested specimen is shown in Fig.10. The surface size of the specimens is 10mm times 10mm.

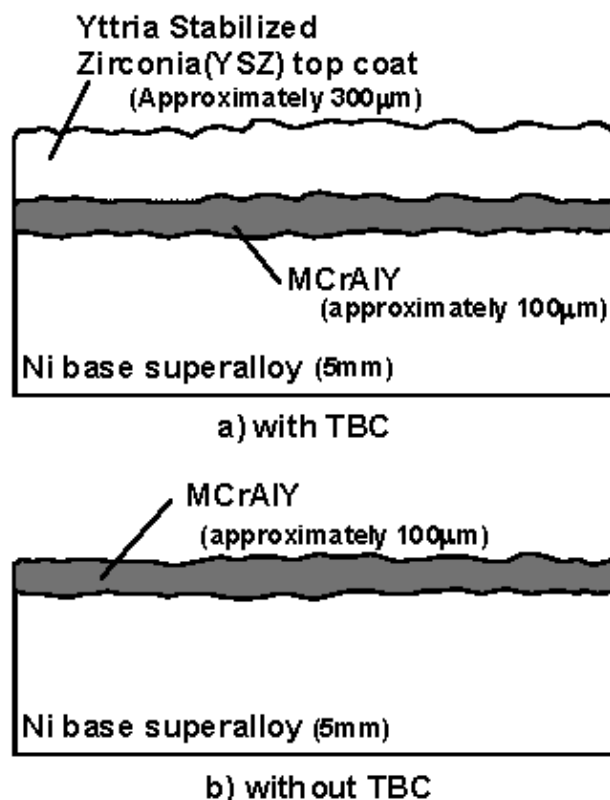


Figure 10. Geometry of cross-section of the tested specimens.

3.1.2. Thermal aging treatments

The two kinds of specimens are aged at 1000°C by using high temperature furnace. The reason for that temperature choice of 1000°C is to simulate the surface temperature of the first rotating blades of state-of-the-art gas turbine plants. The coated specimens (with and without TBC) are aged at 1000°C for various length of times viz, 10, 50, 100, 500, and 1000 hours. Only the specimen with TBC is aged for 3000 hours at 1000°C. The environment is ambient condition. In order to understand the relationship between the aging time and the growth of TGO layer, cross-section of thermally aged specimens is observed by SEM. The thickness of TGO layer for both specimens is measured at 100 points by SEM observations.

3.2. Results and discussion

3.2.1. Characterization for the specimen with TBC

SEM observation gives not only microstructural information but also information of initial degradation such as microcracks, porosities, and TGO. Therefore, cross-sections of TBC and MCrAlY interface for with-TBC specimen are observed by SEM. Typical SEM images of the cross-section of as-received and 3000 hours thermal aged specimen were shown in Fig.2 of the previous section. It is seen that TGO is formed at the TBC/MCrAlY interface. Furthermore, it is concluded, from this figure, that thickness of YSZ layer is almost constant in spite of the prolonged aging time up to 3000 hours. Moreover, TGO layer has irregular shape and variable thickness at the TBC/MCrAlY interface. Typical SEM images of the cross-section around TBC/MCrAlY interface of the specimen aged for 500, 1000, and 3000 hours were shown in Fig.3 of the previous section. It is proven that the TGO layer forms at TBC/MCrAlY interface. This TGO layer contains at least two layers with different color contrast, namely Al_2O_3 , a black layer in this image closer to the bond coating, and mixed oxide, a gray layer in this image closer to YSZ. Furthermore, it is seen from the SEM images that the thickness of the TGO layer increases with the thermal aging time. A close look at the TGO layer reveals that there are many porosities, especially in the mixed oxide. These porosities can be referred to as Kirkendall porosity [14, 15], and they can reduce the adhesive strength of the TBC/MCrAlY interface. [16]

3.2.2. Comparison between the oxide thickness of the specimen with and without TBC

The oxide film thickness variation with aging time is understood from the results of section 2.2.2. However, the effect of TBC on TGO oxidation is not clarified. In order to investigate whether the growth of TGO is accelerated or reduced by TBC, detailed SEM study has been carried out for both specimens. Furthermore, the chemical composition of the TGO layer is determined by a comparison between secondary electron images and backscattered electron images. The results are presented in Fig.11.

For the specimen with TBC, mixed oxide is observed on the entire interface of TBC/MCrAlY. On the other hand, the specimen without TBC contains only island of thin mixed oxide on the surface.

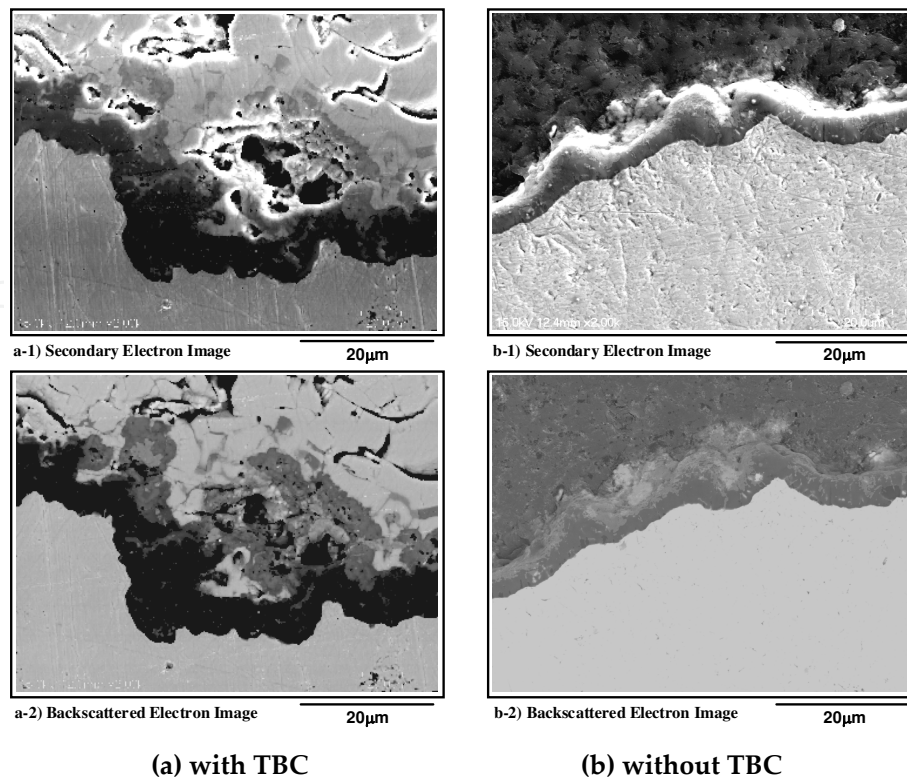


Figure 11. Typical SEM images of the cross sections for the specimens.

The dependence of average thickness of the TGO as a function of aging time for the both specimens is shown in Fig.12. Surprisingly, the TGO thickness of the specimen with TBC is larger than without TBC. It is expected that the average TGO thickness should be smaller for the specimen with TBC with respect to the specimen without TBC. However, the result is quite different. Therefore, SEM analysis to distinguish between the alumina and the mixed oxide layer was carried out.

Comparison between the thickness of each layer of the specimens with and without TBC is performed in Fig.13. It is seen that the alumina thickness is almost same for both specimens. On the other hand, thickness of mixed oxide is quite different in these two cases. Correspondingly, the difference in TGO thickness between the specimens with and without TBC is a result of difference between the mixed oxide thicknesses. The reason why the specimen without TBC has thinner mixed oxide can be that this specimen forms dense TGO due to smaller thermal expansion mismatch stress than the specimen with TBC.

For the specimen without TBC, the thickness of the mixed oxide, x_{mn} and the alumina, x_{av} for the specimen without TBC are expressed as follows:

Mixed oxide layer:

$$x_{mn} = k_{mn} \sqrt{T} = 0.052\sqrt{T} \quad (3)$$

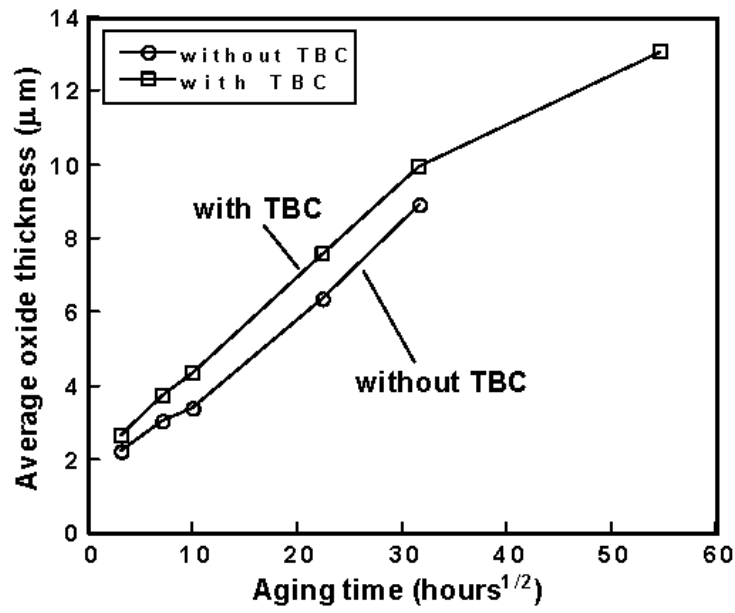


Figure 12. Dependence of the TGO thickness with the aging time for both specimens.

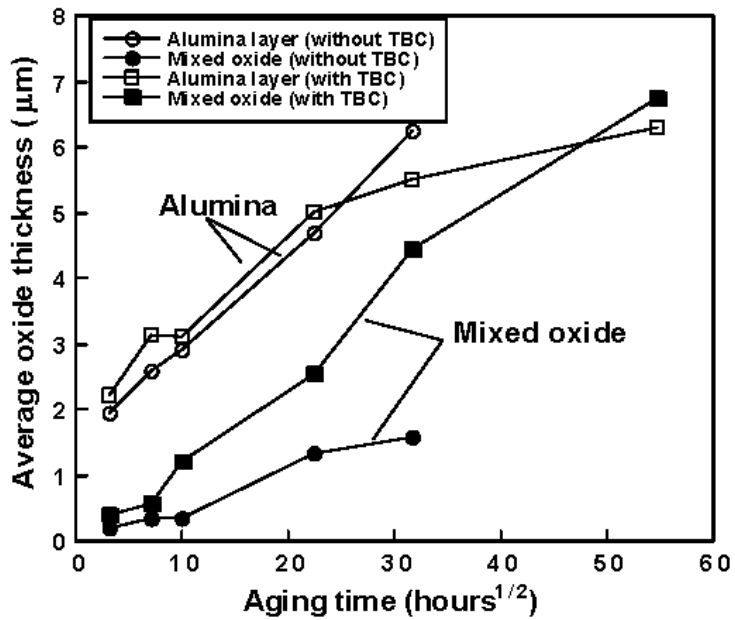


Figure 13. Comparison between the specimen with and without TBC concerning each layer thickness with aging time.

Alumina layer:

$$x_{an} = k_{an} (x_{mn}) \sqrt{T} = 0.232 x_{mn} - 0.497 \times \sqrt{T} \tag{4}$$

where k_{mn} and k_{an} are respectively oxidation rate constant of mixed oxide and alumina for the specimen without TBC.

It is noted the constants in the corresponding oxide film equations with and without TBC are different, as well as that the mixed oxide and the alumina obeyed parabolic law and anomalous parabolic law, respectively for the specimen with TBC. The mixed oxide can enhance on degradation, which indicates that it is beneficial to decrease the thickness of mixed oxide.

3.3. Summary

Owing to understanding the oxidation behavior, a comparison is made between a specimen with TBC and without TBC. A comparison between the specimen with and without TBC shows that TGO is thicker for the specimen with respect to the specimen without TBC. These specimens had different oxidation behavior, which is due to specimen notable growth of mixed oxide for the specimen with TBC. The existence of the TBC has an influence of acceleration on TGO growth. The mixed oxide can enhance on degradation, which indicates that it is beneficial to decrease the thickness of mixed oxide. To do that, we must know the mechanism of TGO growth. Correspondingly, this work is helpful in analyzing mechanisms of TGO growth behavior, and in prolonging TBC life.

4. Effects of Ce and Si additions to CoNiCrAlY bond-coat material on oxidation behavior and bonding strength of thermal barrier coatings

It is generally accepted that the formation of the TGO accelerates TBC failures, and the bonding strength of the TBCs is reduced by the growth of TGO [6]. In section 2, it was indicated that the formation of porosity in a mixed oxide caused stress concentration sites and a decrease in bonding strength. Therefore, inhibition of the TGO formation would be an effective means for improving bonding strength. It is reported that the TGO growth rate depends on chemical composition, existence of atomic-order defects in the bond-coat, top-coat materials etc. [12, 17, 18]. Some approaches, such as modification of the bond-coat or of the coating processes, along with optimization of coating conditions to control the formation of TGO have been considered. In this section, a modified bond-coat material is described, namely adding Ce and Si to a conventional CoNiCrAlY [19].

4.1. Experimental procedure

4.1.1. Used materials

Ni base superalloy, Inconel 601, was used as a substrate material. The substrate was initially grit blasted, and then positioned into a low-pressure plasma spray (LPPS) coating system for several overlaying bond-coats approximately 100 μ m thick. Six different Ce and/or Si added bond-coat materials were developed. The chemical compositions of bond-coat materials were shown in Table 1. In developed powders, Ce contents were in between 0 to 1.5 wt% and Si

conatents were in between 0 to 2 wt%. These Ce and/or Si added bond-coat materials were compared with conventional CoNiCrAlY. A yttria (8 wt%-Y₂O₃) stabilized zirconia (YSZ) TBC top coating approximately 300 μm thick was then applied using an air plasma spraying (APS) coating system.

Bond-coat materials	Chemical compositions (wt%)						
	Co	Ni	Cr	Al	Y	Ce	Si
CoNiCrAlY	Bal.	32	21	8	0.5	-	-
0.5Ce1Si	Bal.	32	21	8	0.5	0.5	1
0.5Ce	Bal.	32	21	8	0.5	0.5	-
0.5Ce2Si	Bal.	32	21	8	0.5	0.5	2
1Si	Bal.	32	21	8	0.5	-	1
1Ce1Si	Bal.	32	21	8	0.5	1	1
1.5Ce1Si	Bal.	32	21	8	0.5	1.5	1

Table 1. Nominal chemical composition and particle size range of spraying powders.

4.1.2. High temperature exposure tests

High temperature exposure tests were performed in 1100°C atmospheric environment inside a muffled furnace. TGO formation was investigated by scanning electron microscopy (SEM) and energy dispersive X-ray spectrometry (EDX) for TBCs with seven different bond-coat materials.

4.1.3. Four-point bending tests

Fig.14 showed a schematic of the four-point bending tests. Specimens, which has dimensions of 40 mm × 5 mm × 4 mm, were aged for 100 and 1000 hours at 1100°C. During the test, an acoustic emission (AE) sensor and a strain gauge measured AE energy and the compressive strain on the specimens' backside, respectively. Assuming that the starting point of a rapid increase in cumulative AE energy corresponds to the occurrence of delamination, bonding strength was evaluated quantitatively by the amount of backside strain at the rapid increase point in cumulative AE energy.

4.2. Results and discussion

4.2.1. High temperature exposure tests

Cross-sectional SEM observation was performed for the TBC coated with several bond-coats aged at 1100°C for 100 hours. Firstly, in order to investigate the influence of Ce and Si additions, TGO morphologies, where located at the top-coat / bond-coat interface, were compared for

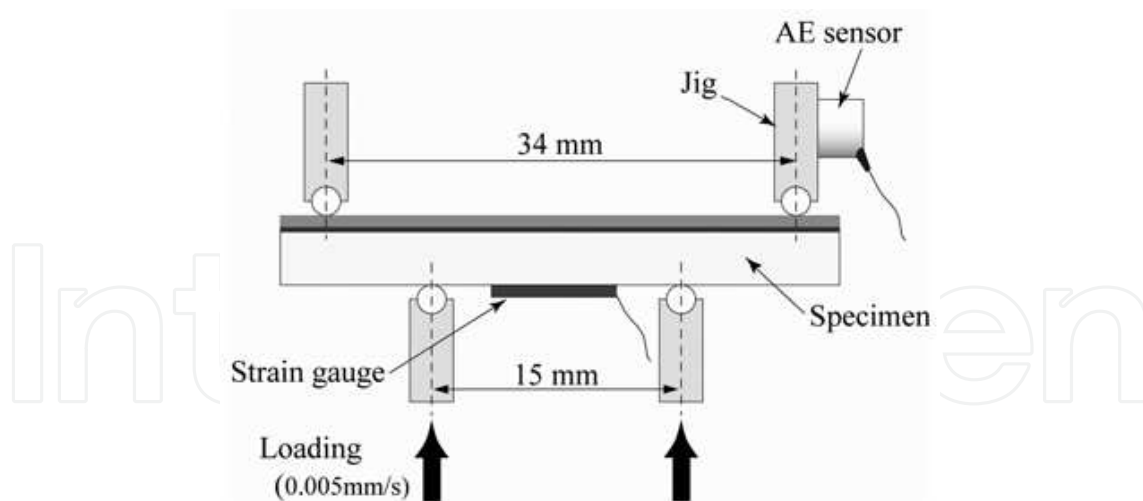


Figure 14. Schematic diagram of four point bending test

TBC coated with CoNiCrAlY, with 1Si, and with 0.5Ce bond-coat materials, and were shown in Fig.15. From these images, mainly a continuous Al_2O_3 film was formed at the interface between YSZ top-coat and bond-coat for all specimens.

In the case of Si addition, the TGO morphology was not changed compared to TBC coated with conventional CoNiCrAlY. In the case of Ce addition, TGO morphology between TBC coated with 0.5Ce bond-coat and the others were completely different. In particular, the formation and the growth of the mixed oxide (gray oxide in SEM images) were different. In the case of a TBC coated with CoNiCrAlY, the mixed oxides formed on the Al_2O_3 . On the other hand, in TBC coated with 1.5Ce1Si bond-coat material, it seems that the mixed oxides grow into the bond-coat. That means that the oxide was interwoven with bond-coat.

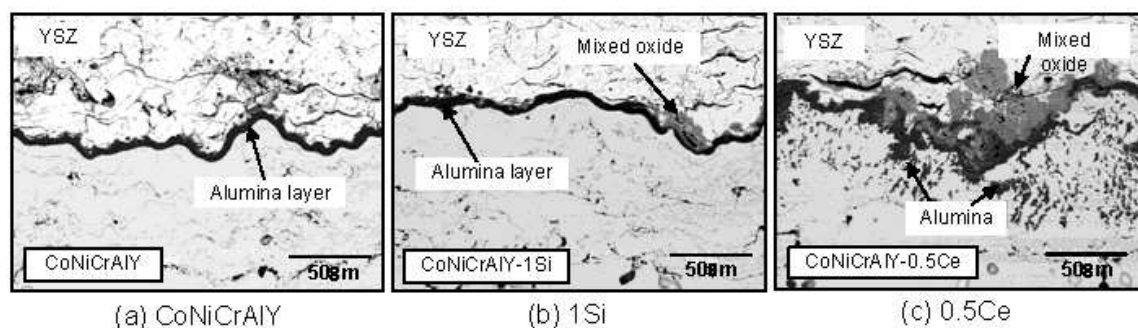


Figure 15. Cross-sectional SEM images of TBCs aged for 100 h at 1100°C. (Effects of separate addition of Si and Ce); (a) CoNiCrAlY, (b) 1Si and (c) 0.5Ce

Secondly, in order to evaluate the amount of Si content, TBCs coated with different Si added bond-coats were compared. Typical SEM images are shown in Fig.16. A significant difference was not shown among the three kinds of TBCs with Si added bond-coats. Accordingly, it is thought that there is almost no effect of Si addition on oxidation behavior.

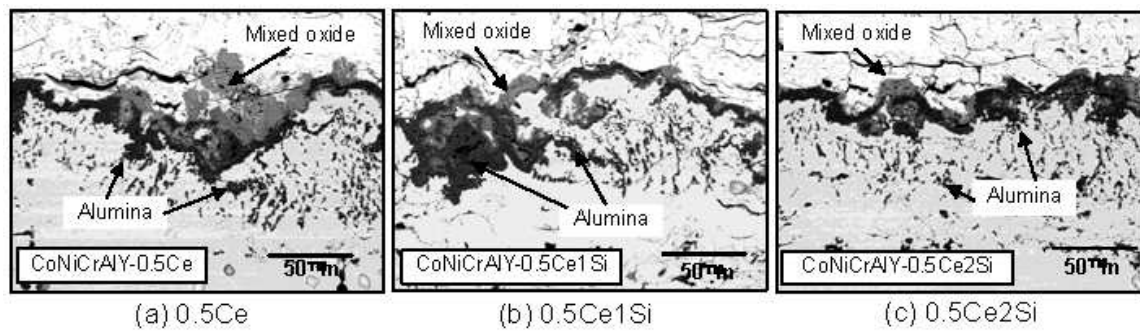


Figure 16. Cross-sectional SEM images of TBCs aged for 100 h at 1100°C. (Effects of variation of Si contents); (a) 0.5Ce, (b) 0.5Ce1Si and (c) 0.5Ce2Si

Furthermore, in order to evaluate the amount of Ce content, TBC coated with several Ce added bond-coat were compared. Typical SEM images are shown in Fig.17. From this figure, internal oxide, hereafter call wedge-like oxide, was observed under the interface. The wedge-like oxide was accelerated by over 1 wt% Ce addition. However, there were not much difference between TBCs coated with 1Ce1Si and 1.5Ce1Si. From these results, growth of the wedge-like oxide was enhanced by Ce addition to the conventional CoNiCrAlY. However, it can be thought that the effect may be saturated with over 1wt% Ce addition.

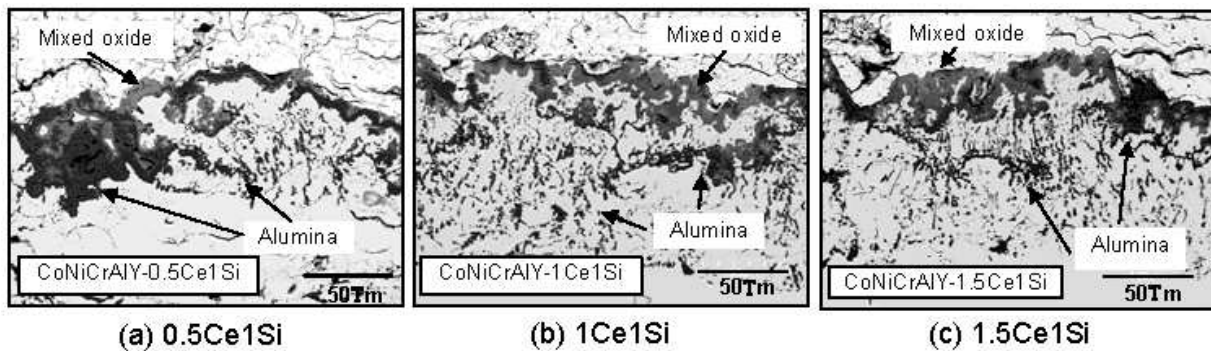


Figure 17. Cross-sectional SEM images of TBCs aged for 100 hours at 1100°C. (Effects of variation of Ce contents)

4.2.2. Mechanisms of formation of wedge-like oxide

From SEM observation, the addition of Ce led to the generation of wedge-like oxide inside the bond-coat. However, the mechanism of wedge-like oxide has not been made clear. Growth process of wedge-like oxide was observed regarding TBC coated with 1.5Ce1Si which showed most remarkable oxide formation. Results of SEM observation results are shown in Fig.18.

As a result, 1 hour aged samples did not observe formation of the wedge-like oxide inside the bond coat. However, the wedge-like oxide started to form after 5 hours aging, and then the thickness of the oxide gradually increased. After 10 hours aging, the wedge-like oxide completely formed inside the bond coat. Due to making clear the mechanism of formation of wedge-like oxide, 1 hour aged sample was observed by energy dispersive X-ray spectroscopy

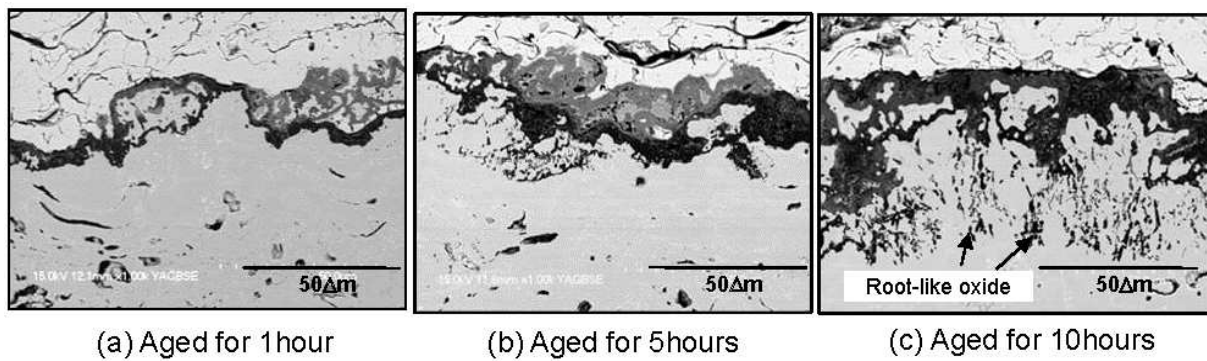


Figure 18. The growth process of wedge-like oxide of TBC coated with 1.5Ce1Si aged at 1100°C.

(EDX). The result of the SEM and the EDX analysis are shown in Fig.19. From SEM image of the figure, there were gray and white regions. In the gray regions, mainly Al and Ni were identified. Therefore, the gray regions can be NiAl intermetallic, namely β -phase. On the other hand, in the white regions, Ce and O were identified by EDX analysis. From this result, Ce-oxide (CeO_2) already existed inside the bond coat at this point. The result indicates that Ce oxidized preferentially rather than Al. From Ellingham diagram, Al oxidized preferentially rather than Ce under 1100°C. However, in this case, opposite result was obtained. The reason can be considered as follows:

Al makes the intermetallic with Ni. The intermetallic is relatively stable. Therefore, Al cannot be easy to oxidize. The solid solubility limit of Ce in CoNiCrAlY is very low. There is a possibility that Ce, which exceeded the solid solubility limit, independently segregated.

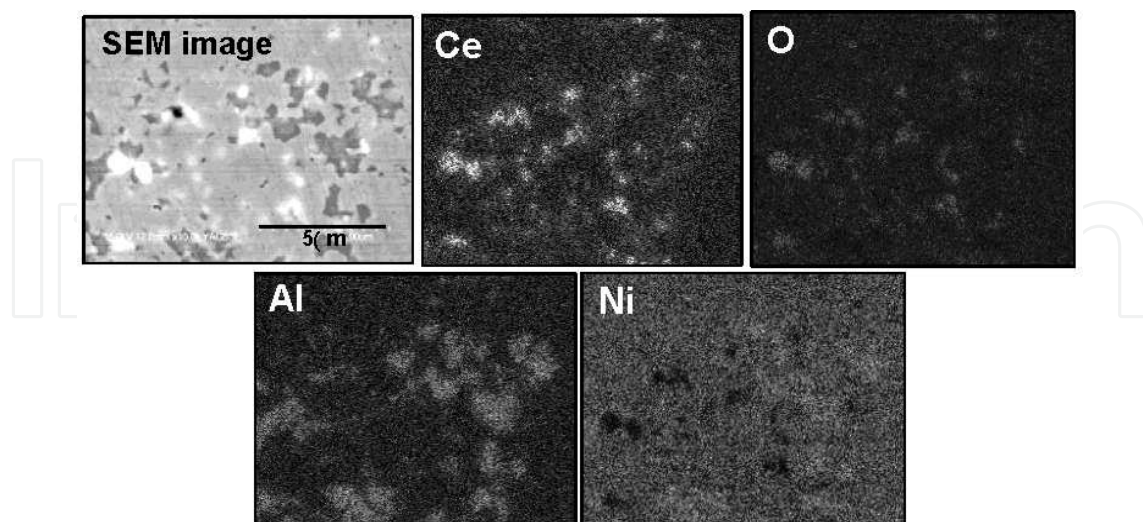


Figure 19. EDX analysis of TBC coated with 1.5Ce1Si aged for 1 hour at 1100°C

And the Ce-oxide, which observed inside bond coat in 1 hour aged sample, can affected oxidation behavior of bond coat. It is known about characteristics of Ce-oxide as follows:

1. Ce-oxide is higher diffusion rate than Al_2O_3 .

- Diffusion rate of O into Al_2O_3 : $D_{\text{Al}_2\text{O}_3} \sim 10^{-15} \sim 10^{-27} \text{ m}^2/\text{s}$ (1000°C) [20]
- Diffusion rate of O into CeO_2 : $D_{\text{CeO}_2} \sim 10^{-8} \sim 10^{-12} \text{ m}^2/\text{s}$ (1100°C) [21]
- Diffusion rate of Al into MCrAlY (12 wt%Al): $D_{\text{Al}} \sim 10^{-14} \text{ m}^2/\text{s}$ (1100°C) [22]

2. Ce has non-stoichiometric property, and has oxygen storage function.

From these characteristics, it is suggested that Ce-oxide can be an oxygen path in bond-coat.

In the case of 5 hours aged sample, the Ni_3Al intermetallic (β -phase) did not recognize inside the bond coat. This means that Al in Ni_3Al oxidized and formed Al_2O_3 . As a result, it can be decreased that Al concentration gradient between the interface and inside of bond-coat, due to decreasing Al concentration in bond-coat. Furthermore, focused on the Al_2O_3 at the interface, the Al_2O_3 was a porous film. Generally, Al_2O_3 was formed densely, and should play a role of oxygen barrier. However, in this case, it can be easy to penetrate oxygen via such porous Al_2O_3 . From the result of observation of 1 hour aged specimen, Ce-oxide was formed diffusion path for oxygen in the bond-coat. Therefore, the Al, which remained in the bond coat, was oxidized at the inside of bond coat. From the results, it is suggested that the oxidation mechanism of the bond coat in case of TBC coated with Ce added bond-coat. The schematic illustration of the TGO formation mechanism is shown in Fig.20.

Due to high temperature exposure, firstly, Ce in the bond-coat was oxidized. And then, Al_2O_3 was formed at the interface between the TBC and the bond-coat. If there is Ni_3Al intermetallic (β -phase) in the bond-coat, diffusion of Al to the interface and growth of Al_2O_3 proceed due to existence of Al concentration gradient. When the β -phase depleted, the diffusion rate of Al to the interface can be decrease. And then, due to formation of porous Al_2O_3 layer at the interface, it is easy to penetrate oxygen to the inside of the bond coat. Moreover, oxygen penetrates deeper through the Ce-oxide. As a result, wedge-like oxide can be formed.

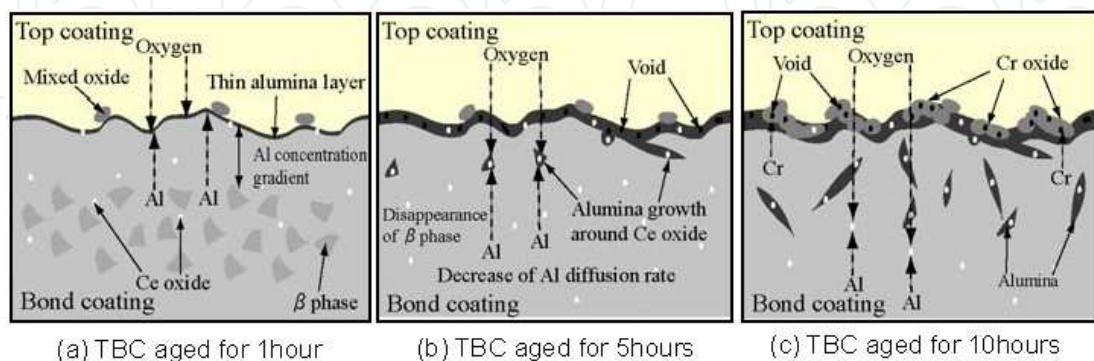


Figure 20. Schematic illustration of the TGO formation mechanism. (In case of TBC with Ce content bond coat aged at 1373 K).

4.2.3. Four-point bending tests

Results of the specimens aged for 100 hours and 1000 hours at 1100°C are shown in Fig.21 (a), (b), respectively.

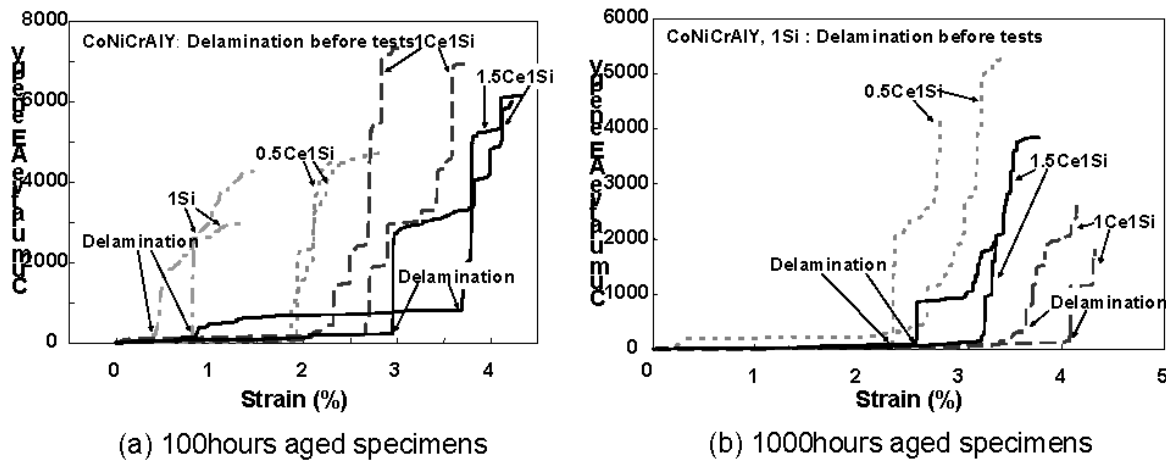


Figure 21. Results of four-point bending tests for the TBCs aged at 1100°C.

In the case of TBC coated with the conventional CoNiCrAlY, delamination occurred during heat treatment. Accordingly, this specimen could not be tested. This result shows that the TBC coated with the conventional CoNiCrAlY has low bonding strength. In case of 100 hours aged specimens, bonding strength increased with increasing Ce addition to the bond-coat. In samples aged for 1000 hours, TBC coated with 1Si delaminated only high temperature exposure. As a result, Si addition cannot be effective for the improvement of the bonding strength. And the TBC coated with 1Ce1Si was the highest bonding strength. In this specimen, the strain value of starting point of delamination was approximately 4%. Normally, due to degradation, the bonding strength gradually decreases. Therefore, it was supposed that the 1000 hours aged TBCs were lower bonding strength than the 100 hours aged TBCs. However, due to addition of Ce, the bonding strength did not drop down. That means effect of Ce addition. When Ce includes over 1wt%, the effect of Ce addition can be saturated. The wedge-like oxide can improve the bonding strength. And in case of the TBCs coated with low Ce added bond-coat, a delamination was mainly observed in the vicinity of the interface. On the other hand, in TBCs with relatively high Ce added bond-coat, a delamination was formed in YSZ top-coat. From the Figs.15-17, Ce addition to the bond-coat drastically changed thermally grown oxide morphologies, namely formation of wedge-like oxide. The wedge-like oxide can improve the bonding strength. It is supposed that the reason of the improvement is an anchor effect.

4.3. Summary

In this section, in order to promote the improvement of bonding strength of the interface between the thermal barrier coating and the bond coating, chemical composition of Ce and Si

added to the conventional CoNiCrAlY powders was investigated. The following conclusions are drawn:

1. By adding Ce and Si to conventional CoNiCrAlY, morphologies of the thermally grown oxide changed drastically. Furthermore, the influence became more pronounced when the amount of Ce increased.
2. Si addition to the conventional CoNiCrAlY cannot be effective for the improvement of the thermally grown oxide morphology and the bonding strength.
3. The bonding strength increased with increasing Ce addition to the bond-coat. Therefore, Ce addition can be effective for the improvement of bonding strength at the interface.
4. In case of TBCs coated with Ce added bond-coat, although high temperature exposure test was performed for a long period of time, the bonding strength did not drop down.
5. Ce addition to the bond-coat made the wedge-like oxide. The wedge-like oxide can improve the bonding strength. It is supposed that the reason of the improvement is an anchor effect.

5. Conclusions

Formation and growth behavior of thermally grown oxide (TGO) at the interface between ceramic thermal barrier coating and metallic bond coating was described.

During thermal aging, a TGO is formed at the TBC/MCrAlY interface. SEM and EDX analysis show that the TGO contains two different oxides. One is alumina closer to the MCrAlY, and the other is mixed oxide closer to the TBC. Thickness of both alumina and mixed oxide increased with aging time. In the case of aged specimen for a long time, the macrocrack was identified everywhere in the TGO. This reason indicates that thermal expansion mismatch accompanied by formation and growth of alumina is one of the driving forces of macrocracks formation. However, the driving force is not only thermal stress but also decrease in adhesive force or formation of stress concentration site caused by formation of porosity or microcrack. Almost all macrocracks passed through the porosity in mixed oxide or microcrack in YSZ layer. It is thought that the delamination or the spalling is initiated and propagated due to an interaction of these degradation factors such as thermal stress, initiation of stress concentration sites, and decreasing adhesive force due to formation and growth of alumina, porosities and microcracks.

And kinetics of TGO growth were obtained. It has been made clear that oxidation behavior of the mixed oxide layer obeys parabolic law. On the other hand, it is thought that the oxidation rate constant of the alumina is a function of thickness of mixed oxide. Consequently, the alumina thickness obeys anomalous parabolic law.

Furthermore, improvement technique for bonding strength between TBC and bond coat was suggested. By adding Ce and Si to conventional CoNiCrAlY, morphologies of the thermally

grown oxide changed drastically. Furthermore, the influence became more pronounced when the amount of Ce increased. Ce addition to the bond-coat made the wedge-like oxide. The wedge-like oxide can improve the bonding strength. From these results, if we can control the morphology of the TGO, we can control the bonding strength between TBC and bond coat.

Acknowledgements

This study was supported in part by the collaboration with Tohoku Electric & Power Co., Ltd. And the author would like to express thanks to Prof. T. Shoji, all of students and staffs in our laboratory, and collaborators involved in this study.

Author details

Kazuhiro Ogawa*

Address all correspondence to: kogawa@rift.mech.tohoku.ac.jp

Fracture and Reliability Research Institute, Tohoku University, Sendai, Japan

References

- [1] Ito S, Saeki H, Inomata A, Ootomo F, Yamashita K, Fukuyama Y, Koda E, Takahashi T, Sato M, Koyama M, Ninomiya T, Conceptual Design and Cooling Blade Development of 1700°C Class High-Temperature Gas Turbine, *Transaction of ASME* 2005; 127 358-368.
- [2] Hirano K, Application of eutectic composites to gas turbine system and fundamental fracture properties up to 1700°C, *Journal of the European Ceramic Society* 2005; 25 1191-1199.
- [3] Meier S.M, Gupta D.K, The Evolution of the Thermal Barrier Coatings in Gas Turbine Engine Application, *Journal of Engineering for Gas Turbines and Power* 1994, 116 250-257.
- [4] Gill B.J, Tucker Jr. R.C, Plasma spray coating processes, *Materials Science & Technology* 1986; 2 207-213.
- [5] Goward G.W., Protective coatings - purpose, role, and design, *Materials Science and Technology* 1986, 2 194-200.
- [6] Ogawa K, Shoji T, Aoki H, Fujita N, Torigoe T, Mechanistic Understanding For Degraded Thermal Barrier Coatings, *JSME international Journal* 2001; 44A(4) 507-513.

- [7] Wu B.C, Chang E, Chao C.H, Tsai M.L, The oxide pecking spalling mechanism and spalling modes of ZrO_2 -8wt% Y_2O_3 /Ni-22Cr-10Al-Y thermal barrier coatings under various operating conditions, *Journal of Materials Science* 1990, 25 1112-1119.
- [8] Wu B.C, Chang E, Chang S.F, Tu D, Degradation Mechanisms of ZrO_2 -8wt% Y_2O_3 / Ni-22Cr-10Al-1Y Thermal Barrier Coatings, *Journal of the American Ceramic Society* 1989, 72 212-218.
- [9] Bartlett A, Maschio R, Failure mechanisms of a zirconia-8wt% Ytria thermal barrier coating, *Journal of the American Ceramic Society* 1995, 78(4) 1018-1024.
- [10] Maier R, Scheuermann C.M, Andrews C.W, Degradation of a Two-Layer Thermal Barrier Coating under Thermal Cycling, *Ceramic Bulletin* 1981, 60(5) 555-560.
- [11] Newaz G.M, Nusier S.Q, Chaudhury Z.A, Damage Accumulation Mechanisms in Thermal Barrier Coatings, *Journal of Engineering Materials and Technology* 1998, 120 149-153.
- [12] Ogawa K, Kato T, Shoji T, Improvement of Interface Bonding strength Between Ceramic Thermal Barrier Coatings and Metallic Bond-coats, *Proceedings of the International Thermal Spray Conference* 2002, 900-904.
- [13] Smeltzer W.W, Oxidation of Aluminum in the Temperature Range 400 °C -600 °C, *Journal of the Electrochemical Society* 1956; 103(4) 209-214.
- [14] Son Y.H, Morrall J.E, The Effect of Composition on Marker Movement and Kirkendall Porosity in Ternary Alloys, *Metallurgical and Materials Transactions A* 1989; 20(11) 2299-2303.
- [15] Nesbitt J.A, Heckel R.W, Interdiffusion in Ni-Rich, Ni-Cr-Al Alloys at 1100 and 1200 deg.C, *Metallurgical and Materials Transactions A* 1987; 18(12) 2061-2073.
- [16] L.Peichl, G.Johner, High-temperature behavior of different coatings in high-performance gas turbines and laboratory tests, *Journal of Vacuum Science & Technology A* 1986; 4 2583-2593.
- [17] Newaz G.M, Nusier S.Q, Chaudhury Z.A, Damage Accumulation Mechanisms in Thermal Barrier Coatings, *Journal of Engineering Materials and Technology* 1998; 120 149-153.
- [18] Choi H, Yoon B, Kim H, Lee C, Isothermal oxidation of air plasma spray NiCrAlY bond-coats, *Surface & Coatings Technology* 2002; 150 297-308.
- [19] Tanno M, Ogawa K, Shoji T, Effect of Cerium and Silicon Additions to MCrAlY on the High-Temperature Oxidation Behavior and Bond Strength of Thermal Barrier Coatings, *Key Engineering Materials* 2004; 261-263 1062-1066.
- [20] Zhu D.M, Miller R.A, Thermal Conductivity and Elastic Modulus Evolution of Thermal Barrier Coatings under High Heat Flux Conditions, *Journal of Thermal Spray Technology* 2000; 9(2) 175-180.

- [21] Eaton H.E, Novak R.C, Sintering Studies of Plasma-Sprayed Zirconia, *Surface Coating and Technology* 1987; 32(1-4) 227-236.
- [22] Chen H.C, Pfender E, Heberlein, Structural Changes in Plasma-Sprayed ZrO_2 Coatings After Hot Isostatic Pressing, *Thin Solid Films* 1997; 293(1-2) 227-235.

IntechOpen

IntechOpen

